

## LETTER TO THE EDITOR

## Critical micelle concentration in three-dimensional lattice models of amphiphiles

Aniket Bhattacharya<sup>1,3</sup> and S D Mahanti<sup>2</sup>

<sup>1</sup> Department of Physics, University of Central Florida, Orlando, FL 32816-2385, USA

<sup>2</sup> Department of Physics and Astronomy, Michigan State University, East Lansing, MI 48824-1116, USA

E-mail: aniket@physics.ucf.edu

Received 10 May 2001, in final form 24 August 2001

Published 28 September 2001

Online at [stacks.iop.org/JPhysCM/13/L861](http://stacks.iop.org/JPhysCM/13/L861)

### Abstract

Amphiphilic molecules with hydrophobic tails and hydrophilic heads form micelles of various shapes and sizes above a minimum threshold concentration known as the critical micelle concentration (CMC). The CMC as well as the size and the shape of the aggregates formed depend on various factors, e.g., the length of the amphiphiles, their internal rigidity, and temperature. In this letter we report the results of a detailed investigation of the dependence of the CMC on temperature for different lattice models of the amphiphilic self-assembly. Ensuring that the CMC can be unambiguously associated with a peak in the heat capacity as a function of the amphiphilic concentration, we show that for the amphiphiles of different lengths and head-to-tail ratios, the CMC decreases rapidly as a function of the chain length, consistently with the experimental results. However, for a given chain length, different lattice models predict that the CMC is always an increasing function of temperature. We point out that these lattice models, although widely used, are inadequate to explain the decrease of the CMC with temperature, seen experimentally for non-ionic surfactants.

There is an increasing interest in understanding the self-assembly properties of amphiphilic molecules [1–4] due to their widespread application in fabricating various devices and moieties at the nanometre length scales. For example, micelle formation through the self-assembly of short hydrocarbon amphiphilic chains is used to prepare both ordered and disordered porous structures with pore sizes of the order of 40 Å [5]. Self-assembly of peptide ribbons or sheets has the potential to be used in drug delivery [6]. More recently, short amphiphilic chains have been used to create a medium with evenly distributed carbon nanotubes [7]. Pattern formations

<sup>3</sup> Author to whom any correspondence should be addressed.

of di-block and tri-block co-polymers are also very well known [8]. Quite naturally, attention needs to be paid to understanding amphiphilic self-assembly in terms of different models with varying degree of coarse graining or complexity.

In this letter, we report the results of a detailed investigation of the dependence of CMC on temperature and chain length carried out in various lattice models that are currently used to study the self-assembly of amphiphiles. We point out that additional features need to be incorporated to make these models more realistic. Traditionally, lattice models have been used to understand the micelle formation and phase separation processes of amphiphilic systems because their inherent simplicity is very appealing as compared to their off-lattice counterparts. These lattice models can be broadly divided into two categories. In the first category, the physical system is mapped onto extended Ising-like models with both bond and site variables [9]. These Ising-like models ignore the internal structure of the individual amphiphiles. However, they have successfully predicted both a closed-loop coexistence curve and the temperature dependence of the CMC observed experimentally for non-ionic surfactants (which are amphiphiles) [10].

It has been demonstrated from simple analytic arguments that the internal structure of the amphiphiles, e.g., head-to-tail ratios, the polarity and effective sizes of the amphiphilic head segments, etc, can dictate the final shapes of the micelles [2]. In a continuum description of the amphiphilic self-assembly, the geometrical features of amphiphiles are taken into account by modelling them as successive hydrophilic (head) and hydrophobic (tail) beads (monomers) connected by bonds and immersed in a solvent. Both the solvent molecules and the individual monomers of the amphiphiles are most often assumed to interact with a Lennard-Jones (LJ) potential. The successive monomers in a given chain interact with an anharmonic spring potential to inhibit disintegration of the chain. A specific choice of the LJ parameters then serves to model an amphiphile of a particular type.

Unlike the Ising-type lattice models, the second category of lattice models, which we discuss here, partly take into account these geometrical structures of the amphiphiles and can be looked at as limiting cases of continuum models. Here an amphiphile made of  $m$  head and  $n$  tail segments connected by  $n + m - 1$  bonds (denoted as  $H_m T_n$ ) is restricted to moving on a lattice with suitably defined interactions between the amphiphiles and with the solvent particles in which they are immersed. The simplest of the lattice models of this type is the Larson model [11], where the interaction parameters are kept to a bare minimum by the special choice where the solvent particles are made of either the head or the tail particles as shown in figure 1(a). As a result, the phase diagram associated with the self-assembly can be explored in terms of a single parameter, namely  $\epsilon_{ht}/(k_B T)$ , where  $\epsilon_{ht}$  is a measure of the strength of the interaction between a head and a tail particle,  $k_B$  is the Boltzmann constant, and  $T$  is the temperature.

In this work we have used a more general model, where the solvent particles are in general different from the head and the tail segments. This model, which has a few additional parameters compared to the Larson model, has been studied extensively by Care and co-workers [12–15] and more recently by us [16]. Both the models capture many of the features of amphiphilic self-assembly. For example, Monte Carlo (MC) simulation showed the existence of lamellar and hexagonal phases and vesicular structures [11–15, 17, 18] in these models. The results obtained from these lattice models have also been compared with those from analytic mean-field theories [16, 19, 20]. It is worth mentioning that in both the Larson model and the Care model, the lattice is completely occupied either with an amphiphilic moiety or with a solvent particle.

In this letter we have introduced a new lattice model where the solvent degrees of freedom are removed in favour of an effective interaction between the amphiphiles. Before we discuss

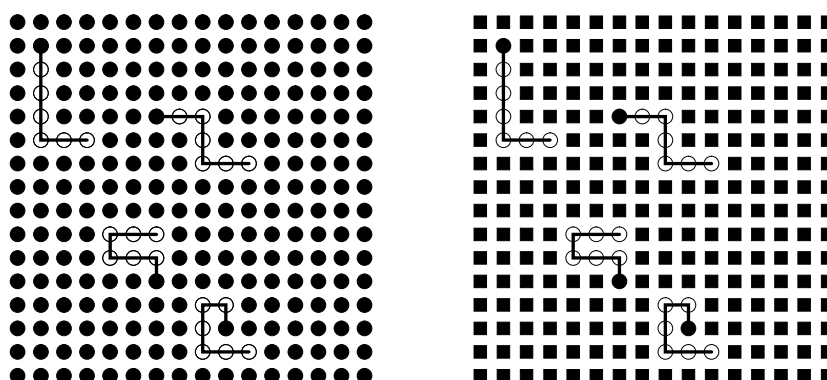


**Figure 1.** (a) The Larson model for  $H_1T_6$ . Each amphiphile is made of one head ( $\bullet$ ) and six tail ( $\circ$ ) monomers connected by six bonds; the solvent particles are chosen to be made of head particles. (b) In the Care model the solvent particles (filled squares) are chosen to be different.

this effective-lattice model, we would like to make a few remarks about the continuum models. Most of the molecular dynamics (MD) simulation studies on continuum models have been carried out for a small number ( $\leq 100$ ) of realistic amphiphilic chains [22–25]. Recently Maillet, Lachet, and Coveney have [26] reported a fully atomistic study of the structure and dynamics of micelles of approximately 50 realistic amphiphiles surrounded by 3000 water molecules, taking into account the relevant long-range interactions and stretching the MD run up to 3 ns. Because of the small concentration of the amphiphiles (relevant for micelle formation), monitoring the solvent degrees of freedom exhausts most of the computer time. This inhibits the study of aggregation properties for a large number of amphiphiles. Naturally, simpler *effective-continuum models* have also been studied through MC and MD simulation where the *solvent degrees of freedom have been eliminated at the cost of effective interaction parameters among amphiphilic segments only*. These off-lattice models without the solvent particles are very enticing for numerical expediency and many of the features are qualitatively similar [27–30]. The lattice versions of these continuum models without the solvent particles (we will refer to them as effective-lattice models (ELM)) have not been studied in the context of amphiphilic self-assembly so far.

The purpose of this letter is twofold. First, we report the self-assembling properties of the amphiphiles in the ELM proposed here and compare the results with those obtained from other lattice models which include the solvent particles explicitly. Second, by carrying out extensive MC simulation for different chain lengths, concentrations, and temperatures on these lattice models, both with and without the solvent particles, we establish an important generic result: *the CMC in the lattice models in this class always increases with increasing temperature*. We point out that this is an obvious limitation of these lattice models because experimental investigations on various amphiphiles show [31] that the CMC for non-ionic surfactants decreases with increasing temperature. We discuss the limitations of these models and suggest further improvements.

First we show the MC simulation results for the Care model where the amphiphiles are confined to a three-dimensional (3D) cubic lattice of size  $L$ . In this model an amphiphile  $H_mT_n$  of length  $(m + n - 1)$  consists of  $m$  hydrophilic heads (H) and  $n$  hydrophobic tails (T) connected by  $m + n - 1$  bonds. We use the notation *unimer* to represent each isolated amphiphile while a *monomer* represents either a head or a tail particle. We consider  $N_A$  of such amphiphiles which occupy  $(m + n)N_A$  lattice sites. The remaining  $N_w = L^3 - (m + n)N_A$

sites are occupied by the solvent particles. The total energy of the system is given by

$$\mathcal{H} = \epsilon_{TS}n_{TS} + \epsilon_{HS}n_{HS} + \epsilon_{HH}n_{HH} + \sum_i \epsilon_c^i \quad (1)$$

where  $n_{TS}$ ,  $n_{HS}$ ,  $n_{HS}$  are the total number of tail–solvent (subscript  $TS$ ), head–solvent (subscript  $HS$ ), and head–head (subscript  $HH$ ) bonds of strengths  $\epsilon_{TS}$ ,  $\epsilon_{HS}$ ,  $\epsilon_{HH}$  respectively and  $\sum_i \epsilon_c^i$  represents the conformation energy which may include bending energies as well. All other interactions  $\epsilon_{HH}$ ,  $\epsilon_{HT}$ , and  $\epsilon_{SS}$  are set to zero. Defining  $\gamma = \epsilon_{HS}/\epsilon_{TS}$  ( $\epsilon_{TS}$  will assumed to be always positive indicating a repulsive interaction between a tail particle of the amphiphile and the solvent),  $\eta = \epsilon_{HH}/\epsilon_{TS}$ ,  $\bar{\epsilon}_i = \epsilon_i/\epsilon_{TS}$ , the above equation can be written as

$$\mathcal{H} = \epsilon_{TS} \left[ n_{TS} + \gamma n_{HS} + \eta n_{HH} + \sum_i \bar{\epsilon}_i \right]. \quad (2)$$

The parameter  $\gamma$  is a measure of hydrophobicity and is crucial in this model. The model exhibits micelle formation and contains many interesting features. Care and co-workers have studied some aspects of this model [12–15] earlier. More recently we have investigated micellar energy and size fluctuations in this model in 2D [16]. Here we explore the properties of this model near the CMC in 3D.

Results of the temperature dependence of the CMC for  $H_1T_2$ ,  $H_1T_3$ , and  $H_2T_4$  are reported here. Simulation details can be found in reference [16]. Figure 2 shows the variation of unimer concentration  $X_1$  (top) and specific heat  $C_v$  (bottom) as a function of the total amphiphilic concentration ( $X$ ) for  $H_1T_2$  (left) and  $H_1T_3$  (right) respectively. We have checked that  $H_2T_4$  also exhibits similar features. The unimer concentration  $X_1$  increases almost linearly until it reaches a maximum value ( $X_1^{max}$ ) occurring at  $X^{max}$ ; with further increase in  $X$ , either  $X_1$  stays at  $X_1^{max}$ , or it saturates to a different value  $X_1^\infty$  around  $X = X^\infty$ . In either case  $X_1^\infty \leq X_1^{max}$  and  $X^\infty \geq X^{max}$ . Both  $X^\infty$  and  $X_1^\infty$  are dependent on the chain length and temperature. Typically one expects the  $X_1$  versus  $X$  plot to look like the one for  $H_1T_2$  at  $T = 0.9$ . Here  $X_1^{max} \sim X_1^\infty$ . However for most of the plots there is a regime ( $X^{max} \leq X \leq X^\infty$ ) where  $X_1$  decreases from  $X_1^{max}$  to its asymptotic value  $X_1^\infty$  as  $X$  increases from  $X_1^{max}$  to  $X^\infty$ . We have checked this

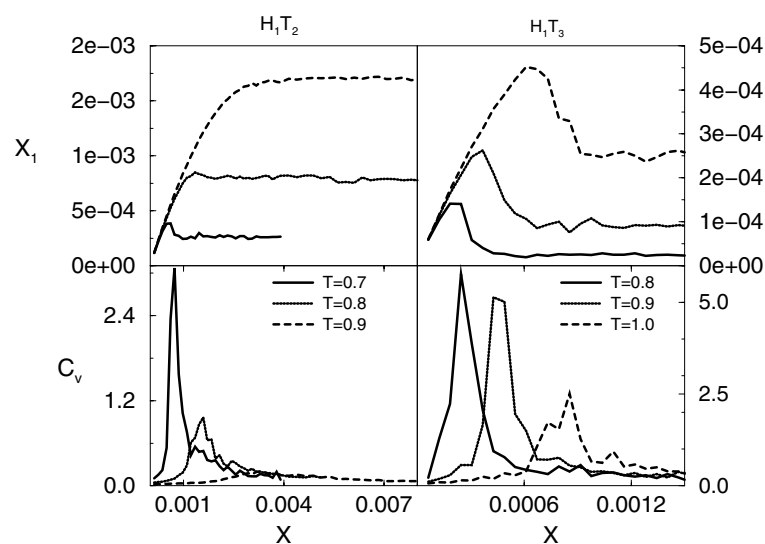


**Figure 2.** Variation of unimer concentration  $X_1$  (top) and specific heat (bottom) as a function of total amphiphilic concentration ( $X$ ) for  $H_1T_2$  (left) and  $H_1T_3$  (right) respectively.

feature by carrying out simulation while approaching this regime,  $X^{max} \leq X \leq X^\infty$ , both from  $X > X^\infty$  and from  $X < X^\infty$ . We get the same result and conclude that this decrease of  $X_1$  in this regime is not an artifact of the simulation.

The physical origin of this initial decrease of  $X_1$  followed by a saturation becomes obvious on looking at the evolution of the cluster distribution (i.e. micellar size distribution) function  $P_n$  as a function of  $X$  in this interval. We find that for  $X < X^{max}$ ,  $P_n$  is a monotonically decreasing function of the micelle size  $n$ . But for  $X \simeq X^{max}$ ,  $P_n$  develops a minimum and a peak. It becomes energetically more favourable for larger clusters to occur even at the expense of lowering of  $X_1$  which causes a slight decrease of  $X_1$ . Beyond  $X^\infty$  the entropy of the unimers prevails over the relative gain in energy for the formation of bigger clusters<sup>4</sup> and the unimer concentration stays roughly the same. One then expects the CMC to lie in the range  $X^{max} \leq X \leq X^\infty$ , which we characterize in the following way.

Figures 2(c) and 2(d) (bottom left and right) show the variation of the specific heat ( $C_v$ ) as a function of  $X$  for  $H_1T_2$  and  $H_1T_3$ .  $C_v$  shows a peak in the region  $X^{max} \leq X \leq X^\infty$ —to be more precise, at  $X \sim X^\infty$ . We have observed similar features for the longer amphiphiles  $H_2T_4$ . From these figures, it is suggestive that the CMC can be identified as being the value of  $X$  where the value of the specific heat is maximum. In order to establish this unambiguously, we have also studied the variation of the specific heat with temperature<sup>5</sup> for fixed  $X$ . Only the results for  $H_1T_3$  are shown in figure 3, although similar results are seen for other chain lengths with different head-to-tail ratios. The peak for  $X = 0.001$  occurs at  $T = 1.04$ . A comparison with figure 2 (bottom right) shows that for  $X = 0.001$  the peak should indeed occur somewhere for  $T > 1.0$ . We show later (figure 6) that the data obtained from the temperature sweep at a fixed  $X = 0.001$  ( $C_v$  peaks at  $T = 1.04$ ) fit well with other sets of data obtained from runs shown in figure 2. Therefore, from these studies it is clear that the temperature variation of the CMC can be obtained quite accurately from the positions of the specific heat peaks. Even from a cursory look at the data shown in figure 2, one can see that for a given chain length the CMC increases with increasing temperature. We will make this statement more quantitative shortly.

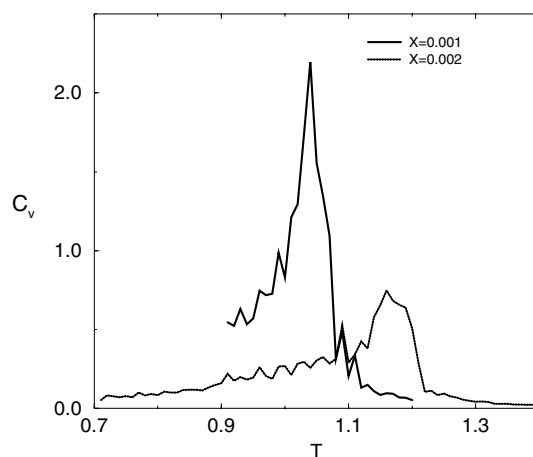


**Figure 3.** Variation of specific heat as a function of temperature ( $T$ ) for  $H_1T_3$ .

<sup>4</sup> This means that the difference in chemical potential ( $\mu_{n+1} - \mu_n$ ) becomes small compared to the entropy of a unimer at a given temperature.

<sup>5</sup> The observed peak as a function of temperature can be explained in terms of a degenerate two-level system and has been discussed in reference [16].

We now discuss the results of a similar investigation for the ELM and demonstrate that this model also contains the same qualitative features. The Hamiltonian for this model can be written as

$$\mathcal{H}_{eff} = \epsilon_{HH} \left[ n_{HH} + n_{HT} + \gamma_{eff} n_{TT} + \sum_i \bar{\epsilon}_c^i \right] \quad (3)$$

where,  $\gamma_{eff} = \epsilon_{TT}/\epsilon_{HH}$ , and  $\bar{\epsilon}_c^i = \epsilon_c^i/\epsilon_{HH}$ . For the sake of comparison of results obtained from the ELM with those from the original model explicitly incorporating the solvent particles (equation (2)), we set the conformation energy terms in both models to be zero ( $\bar{\epsilon}_c^i = \bar{\epsilon}_c^i = 0$ ). We also set  $\epsilon_{HH} = 0$  in equation (2), as is the case for neutral amphiphiles (but not in equation (3) describing the ELM). Equations (2) and (3) simplify to

$$\mathcal{H} = \epsilon_{TS} [n_{TS} + \gamma n_{HS}] \quad (4)$$

$$\mathcal{H}_{eff} = \epsilon_{HH} [n_{HH} + n_{HT} + \gamma_{eff} n_{TT}]. \quad (5)$$

Notice that in both of the models amphiphilicity is introduced in an *ad hoc* fashion through negative values of  $\gamma$  or  $\gamma_{eff}$ , the origin of which lies in the hydrophobic effect. Therefore one would expect the model introduced in this paper (without the explicit presence of solvents) to also qualitatively reproduce the results obtained from the Care or the Larson model.

A rough estimate of energy can be made in order to compare the results obtained from these two models as follows. We look at the energy gain of two amphiphiles as they lie next to each other (forming a dimer) compared to the energy of the two isolated unimers (see figure 4). From the Hamiltonian given by equation (4) (with  $\epsilon_{TS} = 1$ ) and referring to figure 4,  $E_{old} = 2(5\gamma + 13)$  (figure 4(a)),  $E_{new} = 2(5\gamma + 10)$  (figure 4(b)). Therefore  $\Delta E = E_{new} - E_{old} = -6$ , and  $\Delta E/(k_B T) = -6$  for  $k_B T = 1$ . In the ELM, according to equation (5) (with  $\epsilon_{HH} = 1$ ),  $E_{old}^{eff} = 2$ ,  $E_{new}^{eff} = 2 + 3\gamma_{eff}$ ; hence

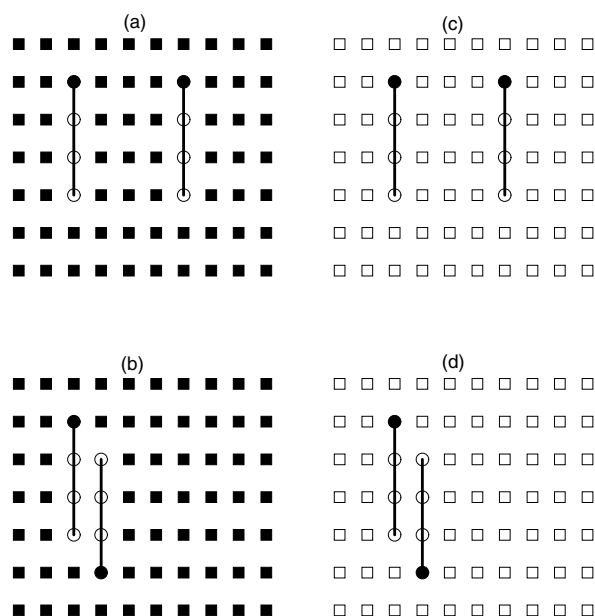


**Figure 4.** Interaction energies of two  $H_1T_3$  amphiphiles; (i) for the model with the solvent according to equation (4) (left); (ii) for the model without the solvent according to equation (5) (right).

$\Delta E^{eff} = E_{new}^{eff} - E_{old}^{eff} = -3\gamma_{eff}$  and  $\Delta E^{eff}/(k_B T) = -3\gamma_{eff}/(k_B T)$ . Therefore, for  $\gamma_{eff} = 1$  and  $k_B T = 0.5$ ,  $\Delta E^{eff}/(k_B T) = -6$ ; the energy difference becomes the same in both models. Hence, keeping all the interaction strengths at unity  $\gamma = \bar{\gamma} = 1$ , we compare the simulation results for  $T = 1.0$  and  $T = 0.5$  for the Hamiltonians of equations (4) and (5) respectively. It is worth pointing out that in obtaining the above energy estimates we have not paid any attention to the entropy of the solvent particles. We will come back to this point in our concluding remarks.

Figure 5 shows the variation of  $X_1$  and the specific heat as a function of the total concentration  $X$  for three different temperatures which are chosen according to the above discussion in order to compare these results with those shown in figure 2. Comparing the results for the temperature 0.5 in figure 5 with those for  $T = 1.0$  in figure 2, we find that the variations of  $X_1$  and  $C_v$  as a function of temperature are indeed qualitatively very similar. It is reassuring that even the slight decrease in the value of  $X_1$  near the CMC is also present in this model. Therefore this effective-lattice model without the solvents also has a CMC, which can be ascertained from the position of the corresponding specific heat peak in the  $X$ - $X_1$  plane. Moreover a comparison of the curves for  $T = 1.0$  in figure 2 with those for  $T = 0.5$  in figure 5 reveals that the magnitudes of  $X_1$  and  $X_{cmc}$  (and hence the positions of the specific heat peak) are very close in these two models.

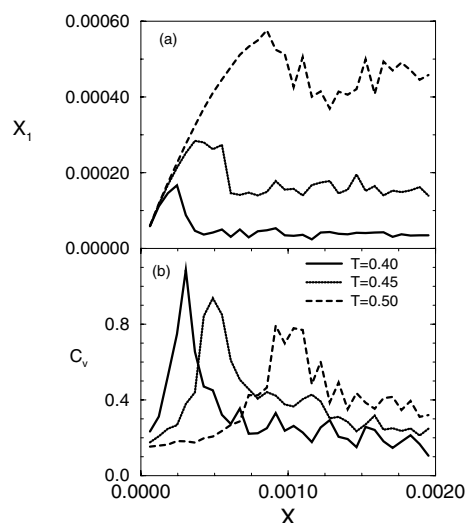


**Figure 5.** Variation of unimer concentration  $X_1$  (top) and specific heat (bottom) as functions of total amphiphilic concentration ( $X$ ) for  $H_1T_3$  for the model without the solvent.

From these detailed investigation of the dependence on  $X$  and  $T$  of  $X_1$  and  $C_v$ , we are now in a position to plot the variation of  $X_{cmc}$  as a function of  $T$  for different amphiphiles obtained in different lattice models. These MC simulation results are summarized in figure 6. The inset shows the same for the effective model for  $H_1T_3$ . From figure 6 it is clear that both the lattice models—one where the solvent particles are explicitly present and the other an effective-lattice model without the explicit presence of the solvent particles—predict an increase in  $X_{cmc}$  with increasing temperature. Moreover, from the absolute value of  $X$  ( $\simeq X_{cmc}$ ) at the CMC we find that the CMC decreases very rapidly with increasing chain length.

The above prediction of the variation of CMC with the chain length seen in lattice models is consistent with experimental results [31]. In contrast, the experimental results

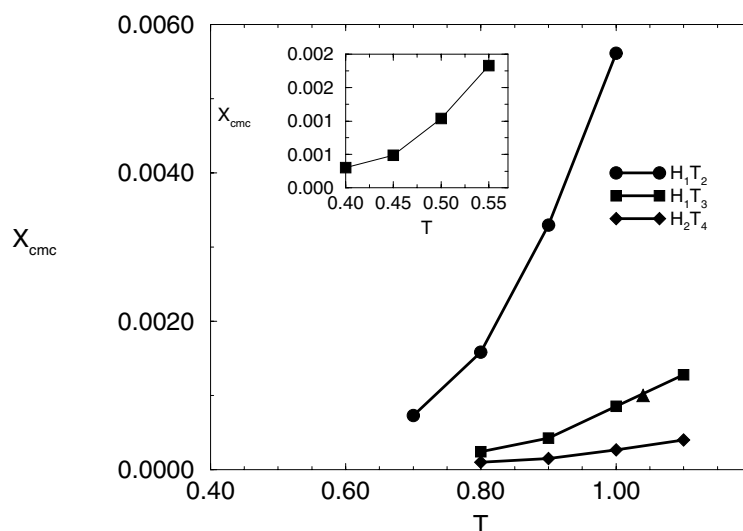


**Figure 6.** Variation of  $X_{cmc}$  as a function of temperature for  $H_1T_2$  (circles),  $H_1T_3$  (squares), and  $H_2T_4$  (diamonds) for the lattice model with solvents. The triangle on the curve for  $H_1T_3$  is taken from a temperature sweep (see the text). The inset shows the same for the effective model for  $H_1T_3$  without the solvent particles.

on the variation of the CMC as a function of temperature for non-ionic surfactant are very different [31]. For example, for non-ionic surfactant, e.g.,  $C_{10}E_5$ , the CMC decreases with increasing temperature, while for polar surfactants, e.g., dodecyl sulphate ( $C_{12}SO_4^-Na^+$ ), after an initial weak decrease the CMC rises as a function of temperature. This different temperature variations of ionic and non-ionic surfactants have been ascribed to the different interfacial structures of the hydrophobic core. A non-ionic micelle has a thick interfacial layer of head groups rather than a sharp transition from the hydrophobic micellar interior to the aqueous bulk seen for the ionic surfactants. Although the lattice models discussed here have been able to predict the phase diagram quite successfully, they are inadequate to capture the temperature dependence of the CMC. The inadequacy lies in the fact that in models of these types, the solvent particles, even when present, do not have any structure. It is worth mentioning that in the effective model without the solvent particles the interaction parameters are in principle functions of all the thermodynamic parameters, e.g., temperature and concentration. Therefore the temperature dependence of the CMC from the effective model does not necessarily reflect a similar temperature dependence from the original model with the solvent particles present. But since the solvents in the actual model are featureless, it is not surprising that the effective model gives a similar qualitative temperature dependence of the CMC.

Finally, it is worth mentioning that the Ising-like model studied by Wenzel *et al* predicts a lowering of the CMC with increasing temperature, and the model also predicts a closed-loop coexistence curve [10]. For a two-component fluid mixture it has been demonstrated by Walker and Vause [32] that a closed-loop coexistence curve will occur because of the competition between the Ising and the orientational degrees of freedom. Evidently, new features need to be added to the lattice models of amphiphiles to account for a closed-loop coexistence curve which in turn will bring out the right temperature dependence of the CMC. Temperature-dependent solute conformation effects have been suggested [31] but have not been incorporated in the large-scale simulations of lattice models. It will be worthwhile to study the properties of the generalized lattice models with additional internal degrees of freedom.



This work at Michigan State University was partially supported by a NSF grant No CHE9903706. We thank the referee for bringing to our attention the work of Maillet *et al* [26]. AB acknowledges a start-up support and a matching grant for equipment from the Office of Sponsored Research at the University of Central Florida and thanks Professor M Schick for discussions.

## References

- [1] DeGiorgio V and Corti M (ed) 1985 *Physics of Amphiphiles: Micelles, Vesicles and Microemulsions* (Amsterdam: North-Holland)
- [2] Israelachvili J N 1985 *Intermolecular and Surface Forces* (New York: Academic)
- [3] Safran S A 1994 *Statistical Thermodynamics of Surfaces, Interfaces and Membranes* (New York: Addison-Wesley)
- [4] Larson R G 1999 *The Structure and Rheology of Complex Fluids* (Oxford: Oxford University Press)
- [5] Kresge C T, Leonowicz M E, Roth W J, Vertuli J C and Beck J S 1992 *Nature* **359** 710  
Tanev P T and Pinnavaia T J 1995 *Science* **267** 865  
McGrath K M, Dabs D M, Yao N, Aksay I A and Gruner S M 1997 *Science* **277** 552
- [6] Matsui H 2000 *J. Phys. Chem. B* **104** 3383
- [7] Vigolo B, Penicaud A, Coulon C, Sauder C, Pailler R, Journet C, Bernier P and Poulin P 2000 *Science* **290** 1331
- [8] Bates F S and Fredrickson G H 1999 *Phys. Today* **52** 32
- [9] Gompper G and Schick M 1994 *Phase Transition and Critical Phenomena* vol 16 (New York: Academic)
- [10] Wenzel W, Ebner C, Jayaprakash C and Pandit R 1989 *J. Phys. C: Solid State Phys.* **1** 4245
- [11] Larson R G, Scriven L E and Davis H T 1985 *J. Chem. Phys.* **83** 2411  
Larson R G 1988 *J. Chem. Phys.* **89** 1642  
Larson R G 1989 *J. Chem. Phys.* **91** 2479  
Larson R G 1992 *J. Chem. Phys.* **96** 7904  
Larson R G 1996 *J. Physique II* **6** 1441
- [12] Care C M 1987 *J. Phys. C: Solid State Phys.* **20** 689
- [13] Care C M 1987 *J. Chem. Soc. Faraday Trans.* **83** 2905
- [14] Brindle D and Care C M 1994 *J. Chem. Soc. Faraday Trans.* **88** 2163
- [15] Desplat J-C and Care C M 1996 *Mol. Phys.* **87** 441
- [16] Bhattacharya A and Mahanti S D 2000 *J. Phys. C: Solid State Phys.* **12** 6141
- [17] Bernardes A T, Henriques V B and Bisch P M 1994 *J. Chem. Phys.* **101** 645
- [18] Bernardes A T 1996 *J. Physique II* **6** 169
- [19] Wijmans C J and Linse P 1995 *J. Phys. Chem.* **11** 3748
- [20] Mackie A D, Panagiotopolous A Z and Szleifer I 1997 *Langmuir* **13** 5022
- [21] Egberts E and Berendsen H J C 1988 *J. Chem. Phys.* **89** 3715
- [22] Rector D R, van Swol F and Henderson J R 1994 *Mol. Phys.* **82** 1009
- [23] Smit B, Esselink K, Hilbers P A, van Os N M, Rupert L A M and Szleifer I 1993 *Langmuir* **9** 9  
Smit B, Hilbers P A, Esselink K, Rupert L A M and van Os N M 1991 *J. Chem. Phys.* **95** 6361
- [24] Palmer B and Liu J 1996 *Langmuir* **12** 746
- [25] Tu K C, Tarek M, Klein M L and Scharf D 1998 *Biophys. J.* **75** 2123  
Tu K C, Klein M L and Tobias D J 1998 *Biophys. J.* **75** 2147
- [26] Maillet J-B, Lachet V and Coveney P V 1999 *Phys. Chem. Chem. Phys.* **1** 5277
- [27] Bhattacharya A, Mahanti S D and Chakrabarti A 1998 *J. Chem. Phys.* **108** 10281
- [28] Nelson P H, Rutledge G C and Hatton T A 1997 *J. Chem. Phys.* **107** 10777
- [29] von Gottberg F K, Smith K A and Hatton T A 1997 *J. Chem. Phys.* **106** 9850
- [30] Milchev A, Bhattacharya A and Binder K 2001 *Macromolecule* **6** 1881
- [31] Jönsson B, Lindman B, Holmberg K and Kronberg B (ed) 1998 *Surfactants and Polymers in Aqueous Solution* (New York: Wiley) chs 2, 4
- [32] Walker J S and Vause C A 1980 *Phys. Lett. A* **79** 421  
Walker J S and Vause C A 1982 *Phys. Lett. A* **90** 419